MONITORING THE DRESSING OPERATION BY ACOUSTIC EMISSION AND ELECTRICAL POWER

Daniela Fernanda Grizzo Moia, dani_fer_nanda@yahoo.com.br [1]
Ícaro Henrique Thomazzella, ihthomazella@hotmail.com [*]
[1] UNESP - Universidade Estadual Paulista, Faculdade de Engenharia – Campus de Bauru – Departamento de Engenharia Mecânica/Elétrica[*] CEP 17033-360 - Bauru – SP

Paulo Roberto de Aguiar[*], aguiarpr@feb.unesp.br [*]
Eduardo Carlos Bianchi[*], bianchi@feb.unesp.br [1]
[1] UNESP - Universidade Estadual Paulista, Faculdade de Engenharia – Campus de Bauru – Departamento de Engenharia Mecânica/Elétrica CEP 17033-360 - Bauru – SP

Abstract: *Grinding is a process used in finishing parts. The excessive friction between the wheel and the ground part makes the tool unsuitable for further use; it is imperative the accomplishment of the process of dressing the grinding wheel to remove or revive the worn out grains of its surface in order to make them suitable for use again. In order to improve such process, this study aimed to conduct an investigation of the dressing operation based on digital processing of signals of acoustic emission and electric power of the drive motor of the wheel, which were collected at a rate of 1 million samples per second. The digital processing of these data was obtained using the Matlab software. Through the experiments it was possible to identify and to control the excessive wear out of the grinding wheel, thereby achieving the characteristics required for machining the part.*

Keywords: *Grinding, Dressing, acoustic emission, electrical power*

1. INTRODUCTION

According to lnasaki et al. (1999), in recent years the machining processes have undergone dramatic changes. It became a permanent tendency to reduce costs, increasing the expectation of high quality products and reducing manufacturing time. The complexity of the grinding process is a result of difficulties encountered in relation to the large number of parameters involved in it. In the grinding process during the machining of the part, there is an excessive friction between the grinding wheel and the rectified part, making the tool inadequate for new use; it is imperative to further the process of dressing the grinding wheel in order to remove or revive the worn out grains of the surface to make them useful again.

The kinematic mechanism of the dressing operation consists in moving the dresser across the grinding wheel in rotation. The penetration of the dresser in a certain dressing depth (ad) implies a breadth of expertise dressing (bd) and this value can be determined by measuring the tip of the dresser with an outline projector, for example (Oliveira et. al ., 2002). The signal processing of acoustic emission (AE) is widely used in grinding process, either for analysis of phenomena occurring in the working part or for studying the cutting tool.

The performance of this process depends mainly on the way the wheel is prepared. The dressing process must produce a design suitable for the grinding, besides the desired profile. The topography of the grinding wheel influences the roughness of the superficial layer of the part through the quantity, the form of the cutting edges of the pore, the volume, and the wearing out behavior of the abrasive layer.

According to Sena, 2007, Marinescu et al., 2007, the dressing operation can be defined as a joint operation of profiling and conventional grinding wheels in the grinding process. The influence of dressing conditions on grinding in its entirety is not well-known, since the geometry of the dresser is a factor of great influence which is not often taken into account. Most studies in the literature uses the depth of dressing (ad), working width (bd), width of the grinding wheel (bs) and the step of dressing (Sd) as variables process. According to Souza (2009), there are two resulting effects from the dressing operation: the macro effect and micro effect. The macro effect is formed due to the shape of the dresser, to the penetration depth and to pitch of dressing in which the operation is held. This phenomenon determines the position in which the edges of the abrasive grains are located. It could be said that the macro effect is the thread (theoretical waving Wt) that the dresser produces on the face of the grinding wheel. The micro effect is formed by the worn out grain pullout (with low anchorage in the league) and fracture of not completely eroded grains, where new cutting edges are generated by the dresser. The aggressiveness of the edges depends on the dressing and on crispness conditions (capacity to form new cutting edges when fractured) of the abrasive grain. The phenomenon of micro effect is therefore related to the type of edge that is formed in the abrasive grains during the dressing operation, varying the aggressiveness of the grinding wheel. Figure 1 shows the scheme of the dressing.

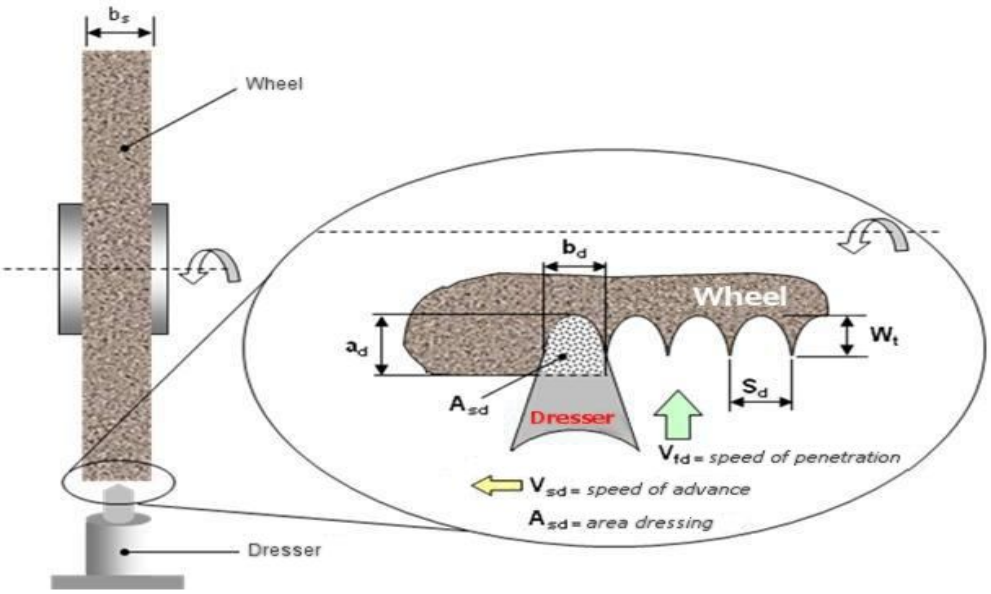

Figure 1. Scheme of the dressing process (adapted from Bianchi, 1990)

According to Paula (2007), the form of sharpening that is normally used, adjusting the advance of the dresser on the basis of its kind, is inadequate because it does not take into account the breadth of the performance in the operation moment. This width still varies due to the wearing out of the dresser tip during several operation dressings. According to Hassui & Diniz (2003), the degree of overlap (Ud) is the relation between the width of performance of the dresser (bd) and the step of dressing (Sd), according to the expression:

$$U_d = \frac{b_d}{S_d} \tag{1}$$

The dressing conditions influence directly the rate of material removal, and also interfere the roughness in the produced part. In thick dressings, where the degree of overlap is small and the number of active edges is also small, an increase in the depth of the grooves is caused, which consequently leads to higher values in roughness. In fine dressing, with higher values of coverage degree, a significantly greater number of active edges divide the efforts and each abrasive grain penetrates less in the part, reducing the values of roughness.

The aim of this research is to conduct an investigation of the dressing operation in the grinding process based on digital processing of acoustic emission signals (pure signal) and electrical power of the drive grinding wheel engine.

2. MATERIALS AND METHODS

Aiming to study the aggressiveness of the grinding wheel when dressed in different degrees of overlap (Ud) and depth of dressing (ad), dressing tests were performed on a flat grinding machine model RAPH - 1055, brand Sulmecânica equipped with a conventional grinding wheel of aluminum oxide from Norton manufacturer (38A220KVS, 355.6 x12, 7x127 mm and maximum speed of 1775 rpm) and using the cutting fluid emulsion with controlled concentration of about 4% of oil volume. A single-point dresser diamond was used, whose dimensions were measured for each test, using a profile projector brand Nikon, model 6C, whose reading accuracy is 1µm.

The layout of the grinding wheel dresser assembly-sensor can be seen in Figure 2.

Figure 2. Schematic assembly of the dressing process with the Acoustic Emission Sensor

Before the beginning of each test, the grinding wheel was worn out by machining a piece of steel without the use of cutting fluid, until the burning part occurred, with the indispensably necessity to perform the grinding wheel dressing operation, which after this process, was worn out and impregnated by chip.

Three tests of aggressiveness throughout each test dressing were conducted: one in the beginning, without the removal of material from the grinding wheel; another in the middle of the test, in which 120 µm of material was removed; and one at the end, with 240 µm of material removed. In these tests, the condition of the aggressiveness in the grinding wheel was assessed through the grinding disc method proposed by Coelho (1991), which consists of submitting a disk under the action of a constant force, the plunge grinding. This is done by using a device similar to a balance of plates placed under the grinding wheel. During the rectification of the disc, its displacement is recorded in time through an electronic probe coupled to the scale capable of providing the offset value in the form of analog voltage. This provides a record of the behavior of the grinding wheel during the grinding under a continuous variation of pressure, provided by the cylindrical shape of the disk. Figure 3 shows the assembly scheme used in this process.

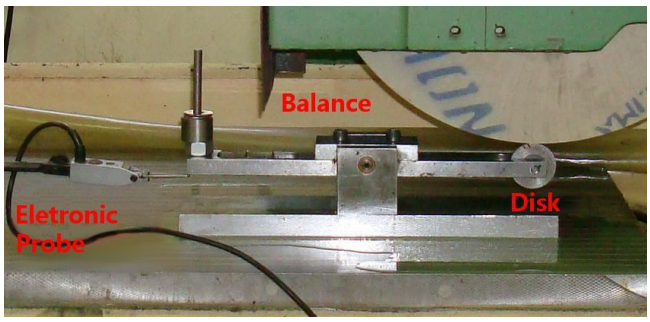

Figure 3. Method of grinding disk

Coelho (1991) relates the disc displacement (δ) versus time (t) by equation 2:

$$\delta(t) = \left(\frac{3}{2} \cdot \frac{K.F_n}{b\sqrt{8r}}.t\right)^{2/3} + \frac{2.\delta_0^{3/2}.b\sqrt{8r}}{K.F_n} \qquad (2)$$

Where:

K = Aggressiveness
Fn = normal force of grinding

b = width of the disc
r = radius of the disc

For this monitoring, signals of electric power of the motor, that drives the grinding wheel, and pure acoustic emission (AE) were collected (with a rate of 1.0 million samples per second), and for the tests of aggression, displacement of the disc (with a rate of 1,000 samples per second) was collected.

In order to acquire electric power signals, a *Hall* effect sensor from manufacturer Nana Electronics Co. Ltd. was used for obtaining the electric current and a piezoelectric sensor, model LV25-P, manufacturer LEM, for obtaining the tension. For the acquisition of Acoustic Emission signals, a piezoelectric sensor manufacturer Sensis was used, coupled to the support of the dresser, connected to a module, also from the manufacturer Sensis which provides as output a signal known as pure or RAW, acoustic emission. To calculate the aggression, the electronic equipment TESATRONIC TT60 was used. Such signals were sent to a data acquisition board from brand National Instruments, model PCI-6111E, with two channels which allows a sampling frequency of 5 MHz divided equally between the channels. This board was installed in a microcomputer, type PC AMD Athlon XP 1.6 GHz, 1 GB of RAM. These data were stored by using the Matlab software. The acquisition module of acoustic emission has been configured according to the parameters shown in Tab. 1.

Table 1 - AE Sensor Setting

Input channel	Input Gain	Gain Signal	Noise Reduction	High Pass Filter	Low Pass Filter
02	60	60	05	50 kHz	None

14 tests were performed in total, of which 12 were used and two were discarded due to problems occurred in their realization. The tests were performed in the following order: 06*, 07, 08, 09, 10, 11*, 12, 06, 05, 04, 11, 01, 02 and 03. The tests showing the mark * are the ones that were discarded. The tests are shown in Tab. 2.

Table 2 - Data from carried out tests

Tests	U_d	a_d (µm)	b_d (µm)	V_d (m/s)	n (RPM)	Diameter of the grinding wheel (mm)	Number of passes
01	2,0	10	152,3	2,2845	334	314,5	24
02	1,5	10	132,3	1,6460	386	314,3	24
03	1,0	10	165,0	4,9500	714	314,0	24
04	2,0	20	188,9	2,8335	412	315,0	12
05	1,5	20	195,6	3,9120	566	315,2	12
06	1,0	20	172,3	5,1690	745	315,5	12
07	2,0	40	136,9	3,5535	515	316,9	06
08	1,5	40	229,0	4,5800	661	316,7	06
09	1,0	40	240,9	7,2270	1038	316,4	06
10	2,0	60	255,2	3,8280	554	316,2	04
11	1,5	60	277,0	5,5400	798	314,8	04
12	1,0	60	254,9	7,6470	1098	315,7	04

3. STATISTICS USED

3.1 RMS Signal AE

In the interval Δt, the RMS value of the pure signal of acoustic emission can be expressed in equation 3 (Liu, 1991, Webster et al., 1996).

$$AE_{RMS} = \sqrt{\frac{1}{T}\int_0^T AE^2(t)\,dt} \qquad (3)$$

where:

T is the integration time
E(t) is the pure signal of acoustic emission

3.2 DPO

Aguiar et al (2002) obtained an indicative parameter for the burning part, called DPO, which consists of the relationship between the standard deviation of the RMS acoustic emission signal and the cutting power per pass of the grinding wheel.

$$DPO = \sigma(AE).\max(\overline{P}) \quad (4)$$

Where:

σ (AE) is the standard deviation of the acoustic emission signal per passes
$\max(\overline{P})$ is the maximum value of the average power in the pass.

3.3 DPKS

The DPKS is calculated through the standard deviation of the acoustic emission multiplied by the sum of the subtracted power from its standard deviation to the fourth power, represented in Eq. (5).

$$DPKS = \left(\sum_{i=1}^{i=m} P_{(i)} - \sigma(\overline{P})^4 \right) * \sigma(AE) \quad (5)$$

where:

i is the index that ranges from 1 to m points of each pass;
m is the number of points of the pass;
P(i) is the instant value of power;
$\sigma(AE)$ is the standard deviation of the RMS acoustic emission of the pass.
$\sigma(P)$ is the standard deviation of average power passes;

3.4 MVD

Processed in the frequency domain, the statistic CFAR of the average deviation value (MVD) is defined as:

$$T_{mvd}(X) = \left| \frac{1}{M} \sum_{k=0}^{M-1} \log\left[\frac{\overline{X}}{X_k} \right] \right| \quad (6)$$

Where X_k is the k^{th} magnitude block of the FFT algorithm square and 2M is the total number of FFT bins. Statistical analysis of MVD has proven to be effective in detecting transients in some applications. The MVD seems to be useful for the detection of burning in the grinding process (WANG et al, 2001).

3.5 Marse

The MARSE statistic, also called metering, is the area measurement in a shape of AE rectified wave, which can be interpreted as the relative amplitude of the signal. Through MARS statistics, one can determine the energy of acoustic emission and this statistic is also sensitive to the duration and amplitude of the signal. (ndt-ed.org, 2008). Figure 4 illustrates the statistic MARSE.

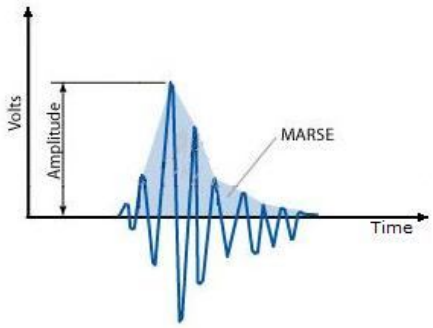

Figure 4. Statistics on the MARSE signal (adapted from Hubbard-ed.org, 2008)

4. RESULTS

The behavior of the statistics observed over all the tests is similar, so only the signal of AE RMS for the test 01will be shown in more details. The graphs relating to these signals can be seen in Fig. 5 and 6.

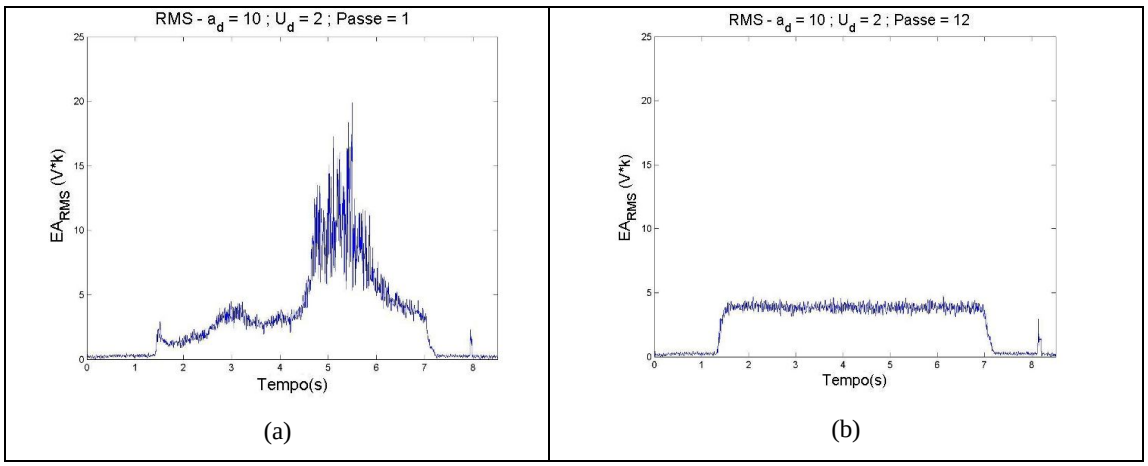

Figure 5. AE RMS referring to passes 1 (a) and 12 (b) of test 1

It is observed, in Fig. 5 (a), that in the first pass the signal is presented with irregularities and high levels especially in the second half of the pass, characterizing irregular and dirty grinding, requiring to be dressed. In Fig. 5 (b), it is noticed that after removing 120 µm of material (12th pass), the signal is presented regularly, featuring the new grinding wheel to be ready for new use.

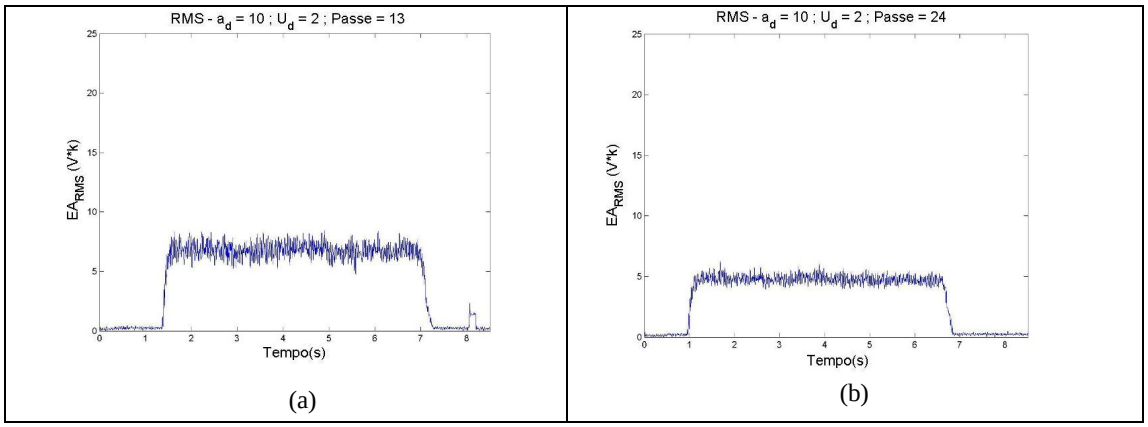

Figure 6. AE RMS referring to passes 13 (a) and 24 (b) of test 1

It is noticed, in Fig. 6 (a), that in the thirteenth pass the signal is presented with some irregularities due to the aggression of the test performed, and such irregularities are no longer found in Fig. 6 (b), in which one can notice that after removing 240 μm of material (24th pass), the signal is presented regularly, featuring the new grinding wheel to be ready for new use.

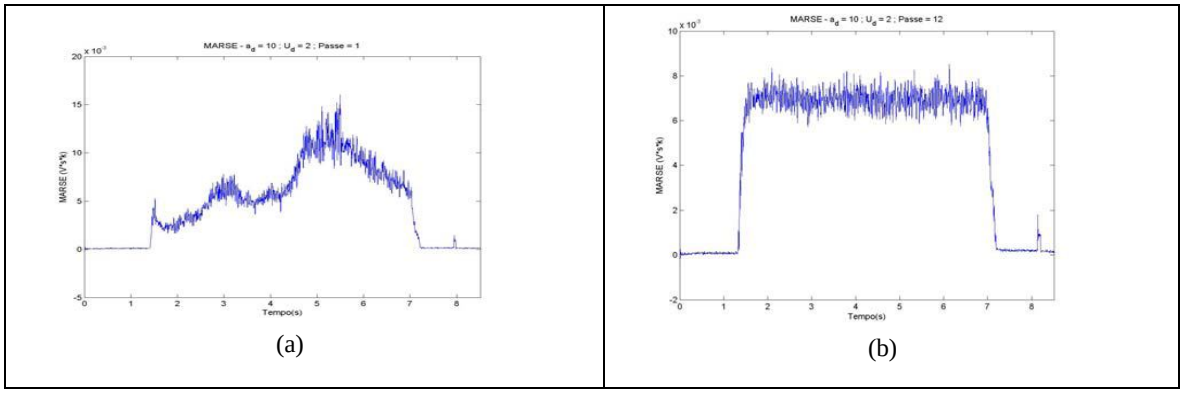

(a) (b)

Figure 7. Marse 1st pass of test 01 and Mars at 12th pass

It is observed in Fig. 7 the graphs of statistics on the MARSE test number 1 in the 1st pass, showing that on the first pass the graph has a behavior similar to MVD statistics graph, and that the grinding wheel is very irregular; as in the pass 12, graph shows up regularly, proving that there are not irregularities in the grinding wheel anymore.

Figure 8 and Figure 9 present the plots of means for AE RMS, electric power, MVD, DPO, and MARSE and DPKS.

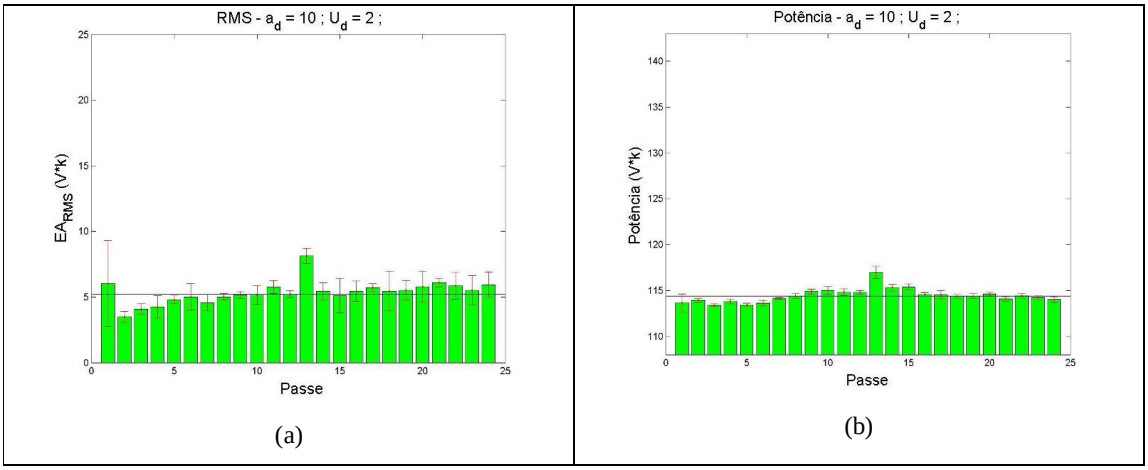

(a) (b)

Figure 8. Averages of (a) EA RMS and (b) electric power in test 1

It is noticed in the graph in Fig. 8 that both signals increased during the test, reaching stability around the tenth pass. The horizontal line represents the total average of the statistic over the passes in the test in question.

It may also be noticed that the passes of number 1 and 13 had higher levels of AE RMS and electric power of the motor, which drives the grinding wheel - this is due to the inaccuracy in placing the grinding wheel for dressing; in this way these passes were excluded from the calculation of the total average in the test.

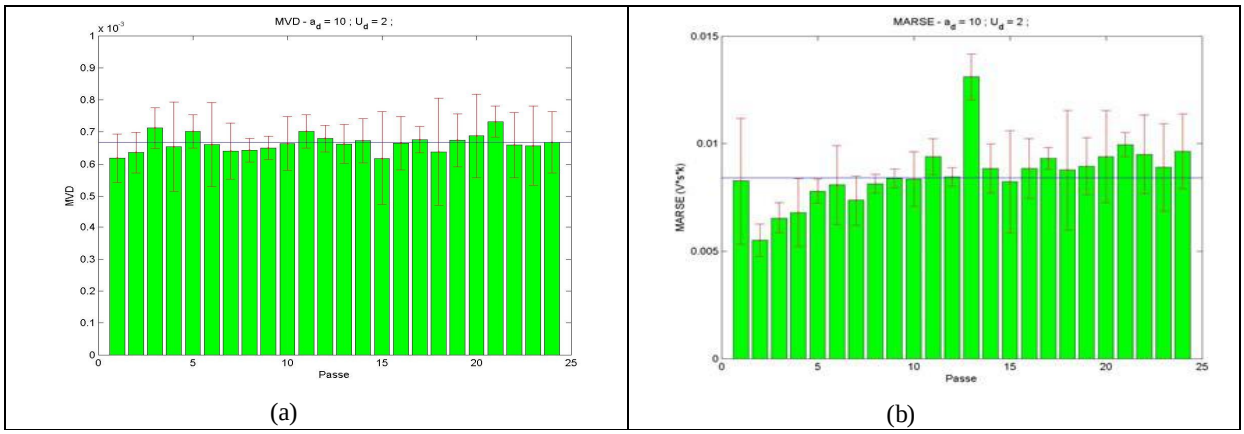

(a) (b)

Figure 9. Average MVD and MARSE in test 1.

It is observed in Fig. 9 that the graph of average MVD is very regular, varying around the overall average value, thus little can be concluded from the graph of average MVD. The graph MARSE seems to be very similar to the one of AE RMS, with wide variations in passes 1 and 13, reaching a stable level in the 10th pass.

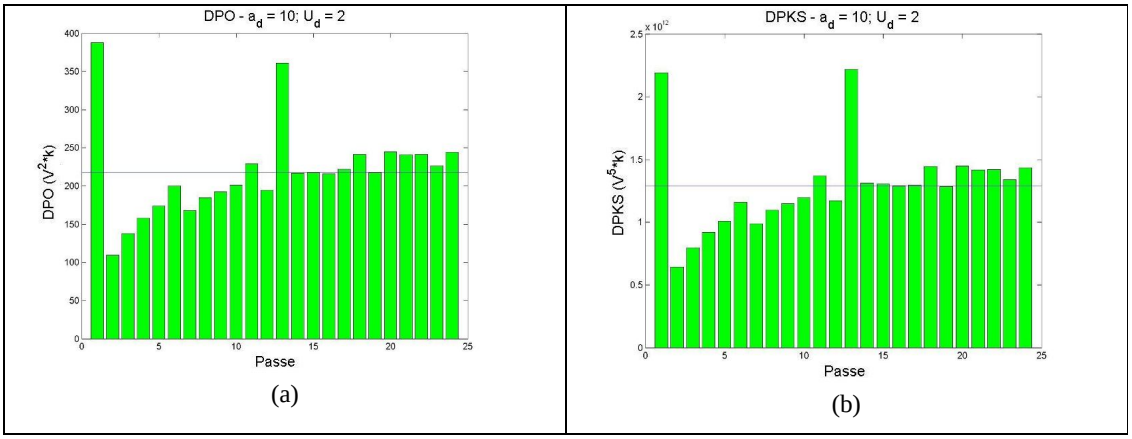

(a) (b)

Figure 10. (a) DPO and (b) DPKS related to test 1

It is observed in the graphs of Fig. 10 that the DPO and DPKS statistics show similar behavior throughout the test and, as in the signal AE RMS, its value increases throughout the test, becoming stable around the 10th pass. From the graphs presented, it can be said that in the 12th pass the grinding wheel was already regular and ready for new use, since the statistics had already been quite regular.

In the other tests, the calculated statistics were similar, with increasing values throughout the test and stabilization just before the half of the test, about 100 μm of removed material.

Aggressivenesses are shown in Fig. 11. The blue bar shows the aggressiveness at the beginning of the study without material removal, the green bar shows the aggressiveness in the half of the test, with 120 μm of removed material, and the red bar shows the aggressiveness at the end of the test with 240 μm of removed material.

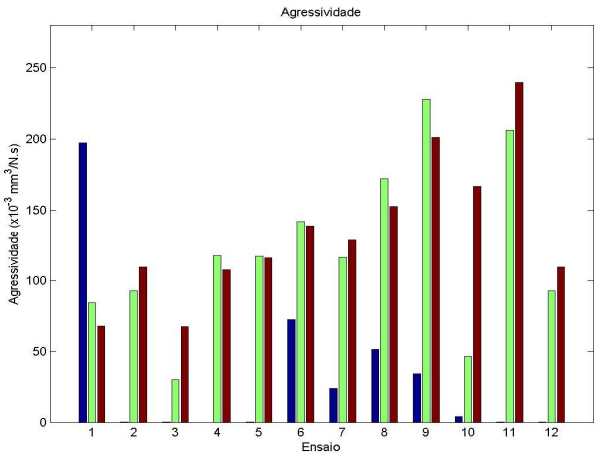

Figure 11. Aggressiveness of grinding wheel during the 12 tests

It is noticed that the last aggressiveness of the grinding wheel (red bar), except for the 10th test, is very close to the aggressiveness in the middle of the test (green bar), showing that with the removal of 120 μm the grinding wheel is already dressed and ready for new use.

Figure 12 shows the spectrum of EA signals from the second and final passes of test 1 in three points, one relating to the beginning of the pass, the other in the half of the pass, and the other at the end of it.

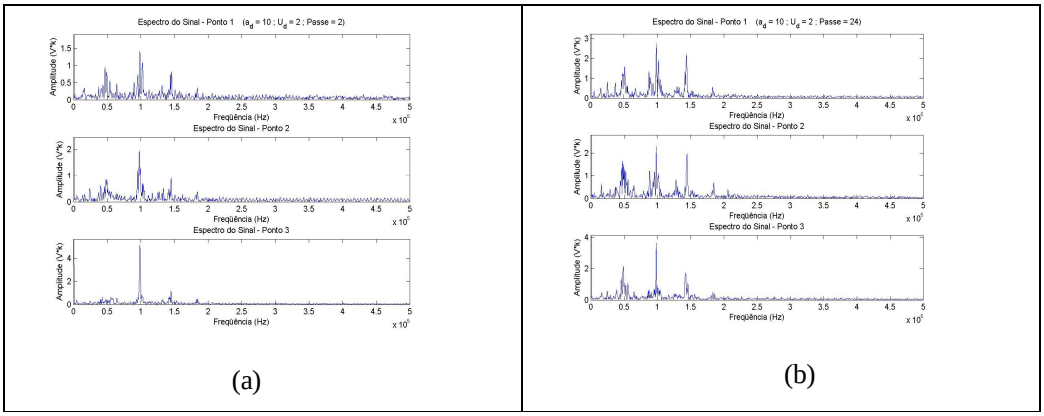

Figure 12. Spectrum of AE signals for the 2nd pass (a) and last pass (b) of test 1

It is noticed, in the graphs of Figure 10, components in the most significant frequency around 50 kHz, 100 kHz and 150 kHz, except for the end of the second pass, in which the components around 50 kHz and 150 kHz showed up with smaller amplitude. It may also be noticed that there is not activity in frequencies over 200 kHz anymore.

The spectrum of AE signals for other passes and other tests was similar to those shown in Figure 12.

5. CONCLUSION

Based on these results, it can be concluded that removing 120 μm of material, the grinding wheel, in most tests, was able to further the use. From the study of the spectrum of AE, one can observe that the components of greater magnitude are around 50 kHz, 100 kHz and 150 kHz. It was also observed that there is not activity at frequencies over 200 kHz anymore, enabling the acquisition of these signals to be made at a lower rate.

It may be noticed that the statistics RMS of AE, MARSE, MVD, DPO and DPKS signals revealed to be good indicators for the control of dressing and, generally, are increased during the process of each test, this could be attributed to the pullout of the worn out grains, with low anchorage in the league, and grain fractures that are not completely eroded, and the irregularity of the grinding wheel in the beginning of the study; while after some passes the grains had a higher anchorage in the league and the grinding wheel was more regular, with increased number of fractures.

It is important to observe that the MVD statistic showed good results in the evaluation of the measurement of the total passes, but the average of the passes presented was very regular, varying around the overall average value, thus little can be concluded from the graph of averages MVD, because it can not be said that the grinding wheel is in good conditions.

The sensor was not sensitive enough to signal power cut, which remained constant, unlike the acoustic emission signal. It was also noticed that the width of the dresser performance (bd), besides the degree of overlap (Ud), had a great influence on the aggressiveness of the grinding wheel, because in the tests with Ud = 2 similar aggressiveness values were obtained in test 06, with Ud = 1 and ad = 20 μm. This is due to the higher values of bd obtained through the increasing dressing depth and due to the conicity of the diamond-tip dresser used.

6. REFERENCES

Aguiar, P. R., Bianchi, E. C. & Oliveira, J. F. G., 2002, “A method for burning detection in grinding process using acoustic emission and effective electrical power signals”, CIRP Journal of Manufacturing Systems, Paris, Vol. 31, No. 3, pp. 253–257.

Bianchi, E. C., 1990, “Terms of action of Dressing in Precision Machining, "Master's thesis submitted to the Engineering School of São Carlos,USP.

Coelho, R.T., 1991, “Experimental study of the depth of dressing in grinding through the grinding disk method in precision machining. São Carlos, EESC, USP, 106 p. Dissertation in Mechanical Engineering. School of Engineering of São Carlos, University de São Paulo.

Hassui, A. & Diniz, A. E.,2003, “Correlating surface roughness and vibration on plunge cylindrical grinding of steel”. International Journal of Machine Tools & Manufacture, vol. 43, pp. 855–862.

Inasaki, I., B. Karpuschewski, M. Wehmeier, 1999 - Grinding Monitoring System Based on Power and Acoustic emission Sensors - Department of System Design Engineering, Keio University, Yokohama-shi, Japan Received on December 20

Liu, J. B., 1991 “Monitoring the precision machining process: Sensors, signal processing and information analysis”, Ph.D. Thesis, University of California at Berkeley, USA.

Marinescu, I. D., Hitchiner, M., Uhlmann, E., Rowe, W. B. & Inasaki, I.,“Handbook of machining with grinding wheels”. 1a. Ed. Boca Raton, FL: CRC Press, Taylor & Francis Group, 2007

NDT RESOURCE CENTER, “Introduction to Acoustic Emission Testing”. Disponível <http://www.ndt-ed.org/index_flash.htm>. Acesso em: 17 de outubro de 2008.

Oliveira, J. F. G., SILVA, E. J., BIFFI M., 2002, "New Architecture Control System for an intelligent High Speed Grinder", Abrasives Magazine – October/November, p. 1-8, 2002.

Paula, W. C. F., 2007 “Surface analysis of parts rectified with the use of artificial neural networks. "Dissertation (Master in Science and Technology of Materials) - University Estadual Paulista - Júlio de Mesquita Filho, Bauru.

Sena, L., “Evaluation of positioning system-slide CNC grinding wheel in a Flexa 600-L with the aid of acoustic emission signals."(Masters in Mechanical Engineering) - University Federal de Santa Catarina, Florianopolis, 2007

Souza, A.G.O.,2009 “Monitoring of dressing in grinding process ”, 2009. 70 f. il

Wang, Z., WILLETT, P., AGUIAR, P. R., WEBSTER, J, 2001, “Neural Network Detection Grinding Burn from Acoustic Emission”. International Journal of Machine tools & Manufacture, volume 41, 2001, pp. 283-309.

WEBSTER, J.; DONG., W. P.; LINDSAY, R. “Raw Acoustic Emission Signal Analysis Of Grinding Process”, In: CIRP, Annals of the CIRP, v.45/1/1195, 1996, p. 335-340.

7. COPYRIGHT